Available online at www.sciencedirect.com
SCIENCE DIRECT®
Journal of Power Sources 119–121 (2003) 2–7
JOURNAL OF POWER SOURCES
www.elsevier.com/locate/jpowsour

On the behavior of different types of graphite anodes

Doron Aurbach*, Hanan Teller, Maxim Koltypin, Elena Levi

Department of Chemistry, Bar-Ilan University, Ramat-Gan 52900, Israel

Abstract

Different types of graphite materials, i.e. synthetic graphite flakes and natural graphite flakes which are used as anode materials in Li-ion batteries were studied. Differences in the electrochemical behavior of electrodes comprised of these materials, mainly in their irreversible capacity, could be correlated to the differences in the particle morphologies and their crystal structure. We propose that graphite particles with a large amount of crevices in their edge planes can crack, due to a build-up of internal pressure as a result of reduction of solution species on the carbon surfaces during the first cathodic polarization on the electrodes. Another important factor determining the electrodes' stability is the existence of some disorder in the particles' structure.

Keywords: Graphite; Particle morphology; Irreversible capacity; AFM; XRD; PC; EC

1. Introduction

Graphite electrodes are widely used as anodes in Li-ion batteries [1]. Graphite intercalates reversibly with lithium in a four-stage process, which involves phase transitions [2]. Since the lithium insertion process into graphite occurs at very low potentials (below 0.3 V versus Li/Li^+), all the relevant solvents and salts in which Li intercalation into graphite may proceed reversibly, are reduced on the graphite electrodes during their cathodic polarization at potentials higher than Li insertion potentials [3], forming passivating surface films on the anodes [4,5]. Graphite electrodes fail in a number of commonly used electrolyte solutions, especially those based on propylene carbonate (PC). A failure mechanism suggested for graphite electrodes in PC solutions relates to an insufficient passivation, which enables co-intercalation of PC molecules with Li-ions into the graphite lattice, causing the exfoliation of the graphene planes (i.e. amorphization of the graphite particles) [6,7]. We have found in recent studies that this mechanism applies to ethereal Li salt solutions [8], whereas in PC solutions the basic 3D structure of the electrodes' active mass remained graphitic (measured by XRD). Our suggestion was that in PC solutions, graphite particles crack due to gas formation. The graphite anodes are thus deactivated due to electrical isolation of the cracked particles by surface films [9].

In this study we tested different kinds of graphite materials in $LiPF_6$/EC–DMC and $LiClO_4$/EC–PC solutions. The differences in behavior of these graphite materials in the latter solution can be explained by the differences in their morphology and structure. The experimental tools for this study included chronopotentiometry (galvanostatic lithiation–delithiation), atomic force microscopy (in situ), electron microscopy, and XRD.

2. Experimental

In this study we used commercial 1 M $LiPF_6$ in an EC:DMC = 1:1 solution from Merck KGaA, Germany. In addition, a solution of 1 M $LiClO_4$ in an EC:PC = 2:3 solution (Tomiyama) was prepared. The water content of these solutions was less than 15 ppm (monitored by Karl Fisher titration, a Metrohm Inc., 562 CF coloumeter). We tested synthetic graphite flakes, KS6, KS15, KS25, and KS44 powders from Timcal Inc., Switzerland, natural graphite flakes (NGF) and another type of natural graphite flake (TNGF) from Chuetso Graphite Works Co. Ltd., Japan. The electrodes were prepared by mixing the active material powder and 10% PVdF binder and adding 1-methyl-2-pyrrolydonen to obtain an homogeneous slurry. The slurry was then spread on a 12 mm diameter pre-rubbed copper disk. The electrodes' mass was usually 4 mg. The electrodes were dried under vacuum for 12 h. A T-shaped cell was used for the galvanostatic measurements, in which a lithium disk was used as a counter electrode. Galvanostatic measurements

* Corresponding author. Fax: +972-3-5351250.
E-mail address: aurbach@mail.biu.ac.il (D. Aurbach).

0378-7753/03/$ – see front matter © 2003 Elsevier Science B.V. All rights reserved.
doi:10.1016/S0378-7753(03)00115-0

were carried out using a MACCOR series 4000 multichannel battery tester at C-rates of C/15 initially (first five cycles) and then at C/7. SEM micrographs were obtained using a JEOL-JSM 840 microscope. XRD measurements were carried out using a Bruker D8 diffractometer. The electrochemical/AFM cells used in this study were described [10]. AFM measurements were carried out using a Topometrix Inc. AFM system, Discoverer Model #2010, with Topometrix pyramidal silicon carbide tips, placed in a special home made glove box [11]. All measurements were conducted at 25 °C.

3. Results and discussion

As was described above, graphite electrodes are widely used as anodes in Li-ion systems. While testing different kinds of graphitic materials such as synthetic and natural graphite flakes in several relevant nonaqueous Li salt solutions (with mixtures of alkyl carbonate solvents), we found that in commonly used solutions such as EC–DMC/$LiPF_6$, there is no big difference in the behavior of the various graphite anodes. However, in EC–PC/$LiClO_4$ solutions there are pronounced differences in the behavior of graphite electrodes comprised of different types of particles in terms of differences in their irreversible capacity (consumed by the film formation processes on the anodes' surfaces). Table 1 summarizes results that were obtained during galvanostatic measurements of cells containing anodes comprised of four different synthetic graphite flakes (KS6-44) and two natural graphite flakes (NGF and TNGF) in EC:PC = 2:3/1 M $LiClO_4$ and in EC:DMC = 1:1/1 M $LiPF_6$ solutions. The specific surface area of the graphite particles and their average size are also listed in Table 1. It is expected that as the graphite particles' surface area increases, the electrodes irreversible capacity should increase as well. This general trend is indeed seen in EC–DMC solutions. However, in contrast, as seen in Table 1, in the EC–PC solutions, as the particle size of the synthetic flakes increases, and hence, their specific surface area decreases, higher irreversible capacity was obtained. These irreversible capacity values are huge, many times higher than the theoretical reversible capacity of graphite (372 mAh/g, corresponding to LiC_6 stoichiometry).

Table 1
a list of the graphite materials that were tested in this study, their average particle size, specific surface area, and irreversible capacity measured in galvanostatic experiments

Name	Specific surface area (BET) (m^2/g)	Particle size (the wide dimension) (μm)	Irreversible capacity (mAh/g)	
			EC–PC $LiClO_4$	EC–DMC $LiPF_6$
KS44	10	45.4[a]	5983	–
KS25	13	27.2[a]	2184	177
KS15	12	17.2[a]	1365	200
KS6	18	6.5[a]	491	175
NGF	8	20[b]	145	126
TNGF	25.9	30[b]	227	–

[a] 90% of the particles are smaller than this value.
[b] Average particle size from SEM observations.

Fig. 1 shows the first and a few consecutive galvanostatic cycles of electrodes comprised of the two natural graphite materials and of one of the synthetic graphite materials (KS25), all in EC:PC = 2:3/1 M $LiClO_4$ solutions. It can easily be seen that the irreversible capacity of the electrodes comprised of natural graphite flakes is much smaller than that of the synthetic graphite electrodes, and

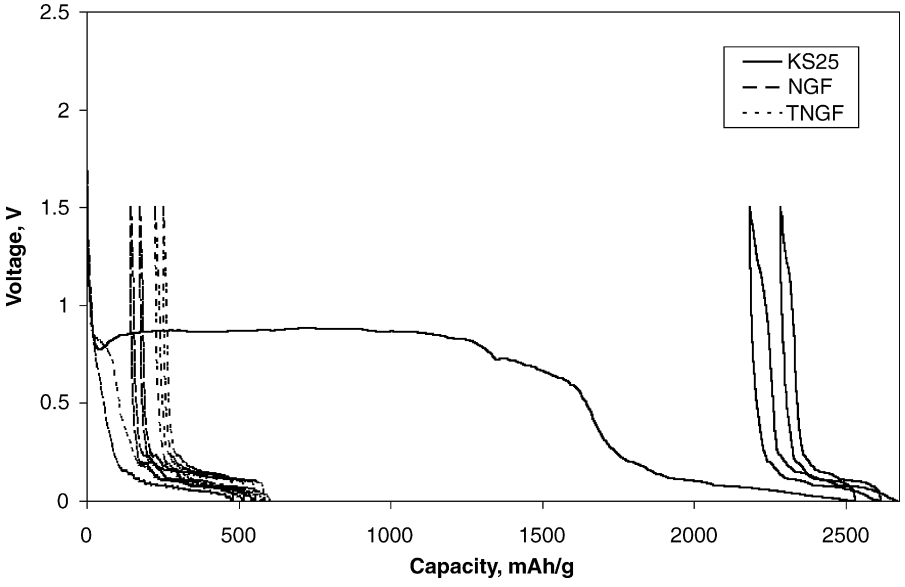

Fig. 1. The first consecutive galvanostatic cycles of electrodes comprised of synthetic graphite flakes (KS25), and natural graphite flakes (NGF and TNGF) in EC:PC = 2:3/1 M $LiClO_4$ solutions.

is only about 50% of the reversible capacity of graphite (see also Table 1).

The difference in behavior between the synthetic graphite electrodes and the natural graphite electrodes may also be seen in Fig. 2, which shows a comparison between representative 2D AFM images and surface height profiles measured in situ at constant potentials during a first cathodic polarization of a synthetic graphite electrode (KS6) and a natural graphite electrode (NGF) in EC:PC = 2:3/1 M $LiClO_4$ solutions. Looking at the images of the KS6 electrode, whose irreversible capacity is the smallest obtained, compared to electrodes comprised of larger synthetic graphite flakes, pronounced morphological changes are observed. The surfaces of the particles at their boundaries are lifted upwards (see the arrows in the images which point to gaps between two particles). In contrast, the images of the NGF electrode show a much smoother passivation process and more stable morphology (compare $\Delta Z_{initial}$, $\Delta Z_{process}$, and $\Delta\Delta Z$ for the two images and profiles, as marked in Fig. 2). The typical height profiles in Fig. 2, show much more pronounced changes due to the cathodic polarization of the synthetic graphite electrodes compared to the electrodes comprised of the natural flakes. The differences in steps on the surface parallel to the basal planes in the KS6 electrodes are about 2.5 times higher than those of the NGF electrode (256 and 100 nm, respectively).

The comparison between the behavior of electrodes comprised of the two different natural graphite materials that we used is also very interesting: it may be seen that although the specific surface area of the TNGF particles is about three times higher than that of the NGF area, yet the irreversible capacity of electrodes based on these materials does not differ very much (Table 1 and Fig. 1). If the major failure mechanism of graphite electrodes and the cause of their irreversible capacity in PC solutions would be due to solvent co-intercalation and exfoliation, we should not see such pronounced differences between the synthetic and natural graphite flakes. Also, the independence of the irreversible capacity on the particles' surface area is striking. Therefore, we suggest a different explanation and attribute the differences in the behavior of the electrodes described above to both morphological and structural differences among the various materials studied.

PC is reduced on the surface of metallic lithium or carbon electrodes at potentials below 1.5 V in the presence of Li-ions to $CH_3CH(OCO_2Li)CH_2OCO_2Li$ and propylene gas [12,13]. The former solid product, which is insoluble in PC solutions, precipitates on the electrodes as surface films. In general, the kinetics of the precipitation process depend both on the cohesion between these $ROCO_2Li$ species and their adhesion to the graphite particles. The $ROCO_2Li$ species are bound to each other and to the graphite surface through the carbonate groups and the Li-ions that bridge between the negatively charged oxygen atoms of the surface species, and between the surface species and the negatively charged carbon atoms. We assume that the methyl group of the PC reduction product interferes badly with the good cohesion and adhesion of the surface species due to its steric hindrance effects. The passivation of carbon electrodes depends on the chance to deposit, as quickly as possible, cohesive and adhesive surface films before competing processes such as co-intercalation of solvent molecules and/or a build-up of internal pressure inside the particles by gas formation take place. The possibility to form protective films should also depend on the morphology of the substrates that are supposed to be passivated, namely, the edge planes of the particles through which Li insertion take place. Fig. 3 shows SEM micrographs of the edge planes (i.e. the planes perpendicular to the basal planes) of KS25, NGF and TNGF particles. We attribute the considerably higher specific surface area of the KS25 particles compared with the NGF particles (although the former particles are thicker, as can be seen in the SEM micrographs) to the high amount of crevices in the edge planes of the synthetic graphite particles. As PC is reduced inside these crevices, and the passivation process is not efficient due to specific characteristics of the precipitating species, the co-product, propylene gas, is trapped inside the crevices forming an internal pressure that eventually cracks the particles. These cracking processes constantly increase the active surface area, leading to enhanced reactions with the solution species, and hence, to the high irreversible capacity of synthetic graphite electrodes. This process is reflected by the surface lifting which was observed in the AFM measurements. As the graphite particles are larger (KS6 < KS15 < KS25 < KS44), the particle thickness increases as well, and hence, there are more crevices at the edge planes, inside which internal pressure can be built up. This explains the differences in the irreversible capacity among the four types of synthetic graphite that were studied (Table 1). When the major solution species reduced is EC (e.g. in mixtures of EC–DMC, EC–DEC, etc.), its solid reduction product $(CH_2OCO_2Li)_2$ forms much more adhesive and cohesive films on the electrodes' surface (compared to the PC reduction product), which block the electron transfer to the solution quickly enough, and hence, stop the reduction process before the build-up of pressure due to the evolution of ethylene gas. This explains the relatively stable behavior of those electrodes regardless of their particle size and morphology in the EC:DMC solution, as shown in Table 1. The natural graphite NGF particles have much smoother edge planes, which contain fewer crevices compared with the synthetic graphite flakes. Thus, the gas bubbles formed during the solution reduction are not trapped inside the crevices, and there is no pronounced internal pressure build-up. Hence, the solid reduction products of PC can precipitate on the electrodes to form surface films, which passivate the electrodes. This leads to the relatively low irreversible capacity of the natural graphite electrodes compared with the synthetic graphite electrodes.

Fig. 4 shows the XRD patterns of synthetic graphite flakes (KS25) and the two natural graphite materials (NGF and

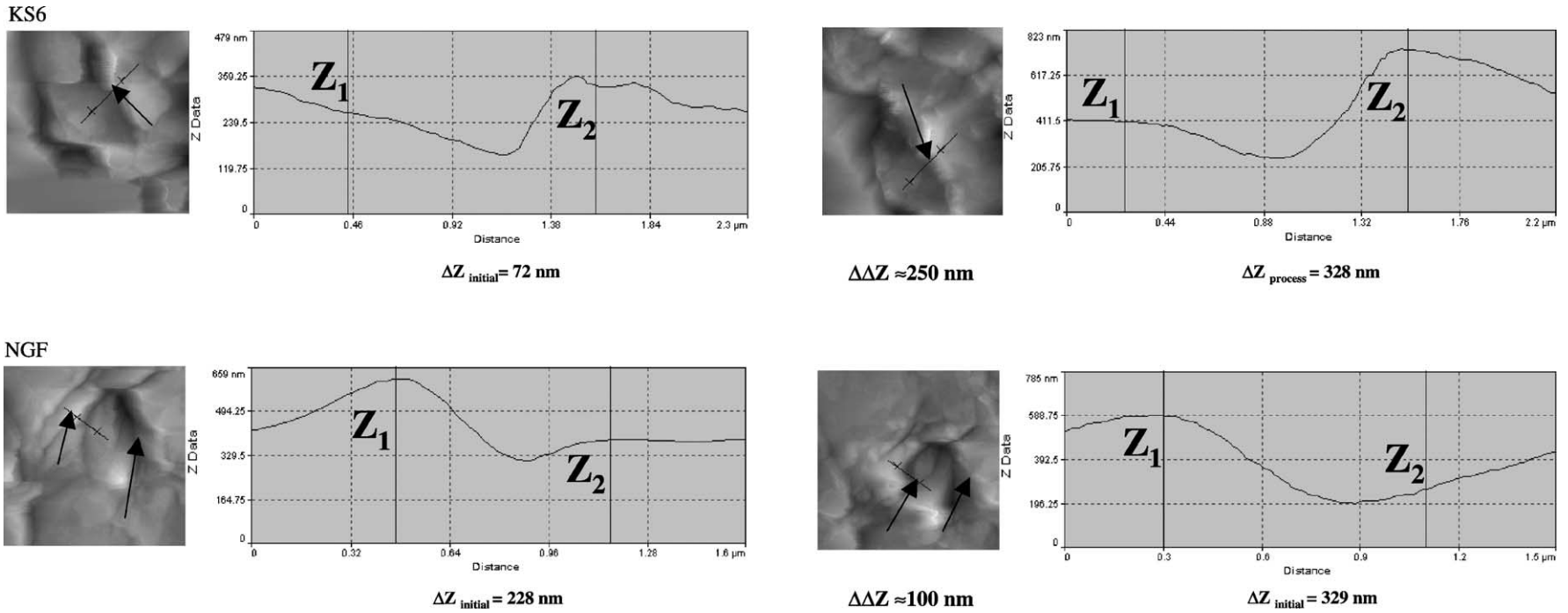

Fig. 2. 2D AFM images of KS6 and NGF electrodes measured in situ during the first galvanostatic cathodic polarization from OCV (≈3 V vs. Li/Li^+) in EC–PC/$LiClO_4$ solutions. The images were obtained at constant potentials that the electrode reached during the process, as indicated. Typical, selected height electrode profiles (ΔZ) are also presented. The height differences in the profiles for the initial and the polarized states are marked. $\Delta\Delta Z$ values marked near the images are the differences in ΔZ between the initial and polarized states.

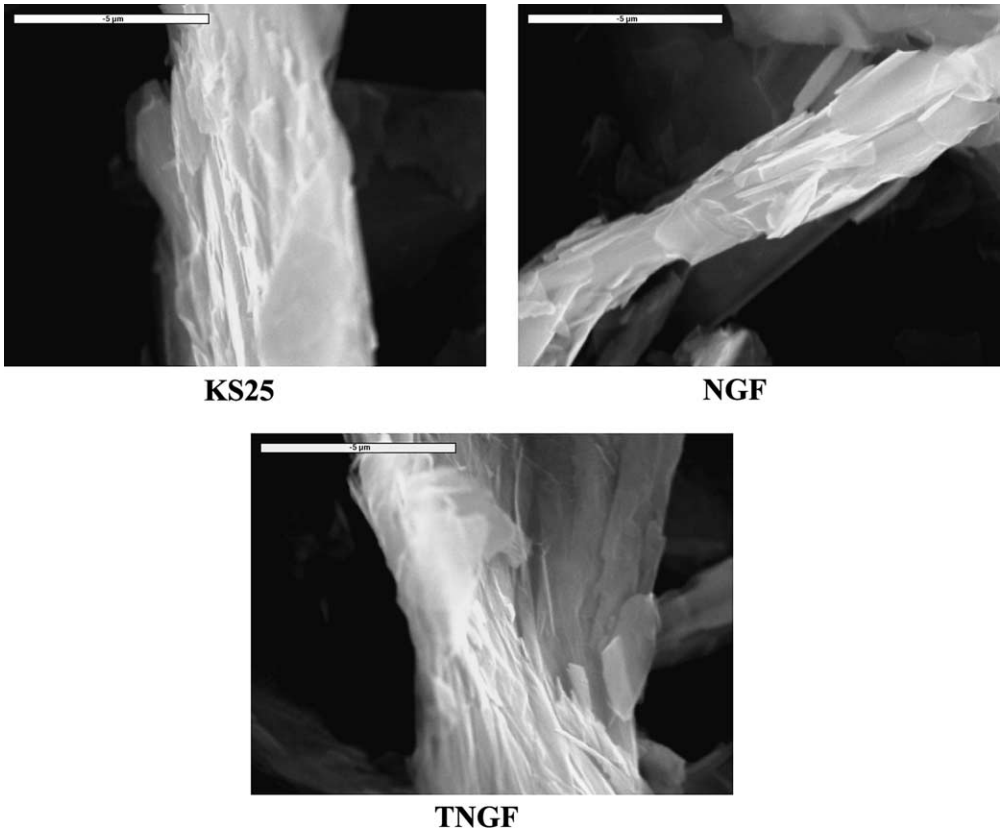

Fig. 3. SEM micrographs of KS25, NGF and TNGF particles (the scale is indicated in each micrograph).

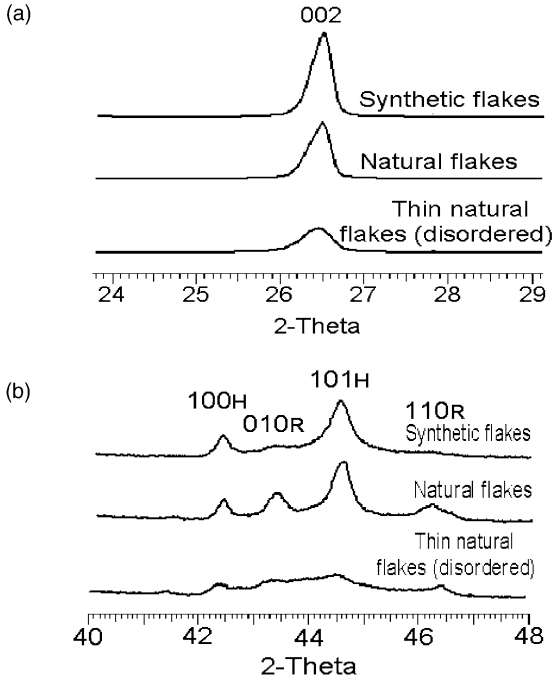

Fig. 4. XRD patterns of synthetic graphite flakes (KS25), natural graphite flakes (NGF), and disordered thin natural graphite flakes (TNGF): (a) the main diffraction peak of graphite (002); (b) characteristic diffraction peaks of the hexagonal and the rhombohedral phases of the graphite particles at higher values of 2θ.

TNGF). All the XRD patterns are typical of graphitic materials comprised of graphene planes bound to each other in weak π bonds to form highly oriented layered structure [14]. However, there are some differences among these samples which are related to the fine structure of the materials and reflect some differences in their degree of order. It may be seen that the KS25 and the NGF materials do not differ too much in their degree of crystallinity. The difference in the intensity of the diffraction peaks is related to the different phase compositions: hexagonal graphite and rhombohedral graphite of these materials, as can be seen by comparing the integral intensities of the diffraction peaks related to those two phases in Fig. 4b. The TNGF XRD patterns show broadening of all the diffraction peaks. As is well known from the diffraction theory, this broadening of the peaks reflects the distortion of the crystal structure due to small crystallite sizes and microstress. Addition of some disorder or distortion into the highly ordered graphite structure adds some stability to the carbon particles, as can be seen with disordered carbons electrodes which are less sensitive to the solution composition in terms of stability, irreversible capacity, etc. Hence, in spite of their high surface area and rough morphology, which are similar to those of the synthetic graphite flakes (see Fig. 3), the TNGF electrodes show high stability and low irreversible capacity even in PC-containing solutions. This is due to the existence

of some disorder in their structure, which prevents the cracking of the particles along their basal planes.

Co-intercalation behavior of solvent into graphite, and other instability problems of these materials, should also be influenced by the crystallinity of graphite. Hence, the destruction of graphite, as described herein, is not likely to occur for lower crystallized carbonaceous materials. Therefore, processes such as solvent co-intercalation can be regulated by graphite electrodes with lower crystallinity. As is obvious from Fig. 4, the degree of crystallinity is in the order of synthetic flakes > natural flakes > thin flakes. This order is quite the same with the order of the irreversible capacities.

It is clear that in future work it will be important to also focus attention on the crystallinity of graphitic materials, especially at the edge planes, and to correlate the degree of crystallinity to the irreversible capacity.

4. Conclusion

In solutions comprising EC and linear alkyl carbonates (DMC, DEC), all graphite electrodes behave similarly and reversibly, while in all pure PC solutions all graphite electrodes fail. In EC–PC/$LiClO_4$ solutions, there is a delicate balance between the possibility to precipitate highly passivating surface films, and hence, to operate the electrodes at low irreversible capacity, and the existence of detrimental processes, which compete with the passivation processes and increase the irreversible capacity. Thereby, fine details such as particles morphology and 3D structure may attenuate this balance, and hence, pronounced differences in behavior, especially in the irreversible capacity, are observed with graphite electrodes comprising different types of particles. Based on electrochemical, XRD, and in situ AFM measurements of graphite electrodes, we converged to the following conclusions.

- The failure mechanism of graphite electrodes in PC solutions involves a build-up of internal pressure, which cracks the particles. This increases their active surface area, allowing intensive electrode-solution irreversible reactions to take place, i.e. it is hard to achieve passivation quickly. The pressure build-up should be attributed to the fact that PC reduction forms propylene gas in addition to solid surface species ($ROCO_2Li$).
- Synthetic graphite particles have a lot of crevices in their edge planes, and thereby, the build-up of internal pressure is pronounced due to PC reduction inside these crevices. Hence, with graphite electrodes comprised of particles with smoother edge planes (e.g. natural graphite flakes), the above detrimental processes are less pronounced and the irreversible capacity measured is relatively small.
- Even in cases of graphite particles with a 'problematic' morphology, the more disordered their 3D structure, the more stable is the behavior of the electrodes. This is because the existence of some disorder adds some strength to the particles and decreases their fragility. Hence, cracking due to a build-up of internal pressure is more difficult in this case, and thereby, the irreversible capacity is small.

References

[1] M. Noel, R. Santhanam, J. Power Sources 72 (1998) 53.
[2] J.R. Dahn, A.K. Sleight, H. Shi, J.N. Reimers, Q. Zhong, B.M. Way, Electrochem. Acta 38 (1993) 1179.
[3] D. Aurbach, Y. Gofer, in: D. Aurbach (Ed.), Nonaqueous Electrochemistry, Marcel Decker, New York, 1999 (Chapter 4).
[4] D. Aurbach, Y. Ein-Eli, B. Markovsky, Y. Carmeli, H. Yamin, S. Luski, Electrochim. Acta 39 (1994) 2559.
[5] M. Winter, P. Novák, A. Monnier, J. Electrochem. Soc. 145 (1998) 428.
[6] J.M. Rosoken, F. Decker, J. Electrochem. Soc. 143 (1996) 2417.
[7] M. Winter, J.O. Besenhard, M.E. Spahr, P. Novak, Adv. Mater. 10 (1998) 725.
[8] D. Aurbach, B. Markovsky, K. Gamolsky, E. Levi, Y. Ein-Eli, Electrochim. Acta 45 (1999) 67.
[9] D.Aurbach.M.D. Levi, E. Levi, A. Schechter, J. Phys. Chem. B 101 (1997) 2195.
[10] D. Aurbach, Y. Cohen, J. Electrochem. Soc. 143 (1996) 3525.
[11] Y. Cohen, D. Aurbach, Rev. Sci. Instrum. 70 (1999) 4668.
[12] D. Aurbach, M. Moshkovichm, Y. Gofer, J. Electrochem. Soc. 148 (2001) E155.
[13] D. Aurbach, H. Gottlieb, Electrochim. Acta 34 (1989) 141.
[14] R.W.G. Wyckoff, Crystal Structures, vol. 1, second ed., Wiley, New York, 1965, pp. 27–29.